



BRNO UNIVERSITY OF TECHNOLOGY

VYSOKÉ UČENÍ TECHNICKÉ V BRNĚ

FACULTY OF CIVIL ENGINEERING

FAKULTA STAVEBNÍ

**HEAT TRANSFER ANALYSIS OF PHASE-CHANGE
PROCESS IN TUBULAR EXCHANGER**

ANALÝZA PŘENOSU TEPLA PŘI FÁZOVÉ ZMĚNĚ
V TRUBKOVÉM VÝMĚNÍKU

STUDENT

STUDENT

ING. TOMÁŠ FEČER

SUPERVISOR

ŠKOLITEL

ING. JOSEF PLÁŠEK, PH.D.

BRNO 2021

Abstract

The system HVAC is frequently based on cyclic phase change of boiling fluid. This phase change of boiling fluid (liquid-gas or gas-liquid) is coupled with boiling heat transfer by nucleate boiling, convective boiling and pre/post dryout effect. The nucleate boiling is depended on superheat of wall (i.e. heat flux) and presence of active nucleation sites. The two-phase convection boiling with dependence on mass flux and vapour quality is performed in liquid film between superheated wall and vapour core. The pre/post dryout effect is significant, when the liquid film is consumed and superheated wall is exposed directly to vapour core. This boiling heat transfer by nucleate boiling, convective boiling and pre/post dryout effect is simplified for engineering design on boiling heat transfer coefficient. Therefore, the dissertation thesis is aimed at experimental analysis of phase-change process in advanced engineering design.

Keywords: evaporation; condensation; water steam; refrigerant

Content

1. Introduction.....	4
2. Boiling Heat Transfer.....	5
2.1. <i>Effect of Mass flux and Heat flux.....</i>	5
2.2. <i>Effect of Inclination angle.....</i>	6
2.3. <i>Effect of Inner diameter.....</i>	7
2.4. <i>Effect of Surface modification.....</i>	8
3. Research Aim.....	9
4. Condensation	10
4.1. <i>Experimental Measurement.....</i>	11
4.2. <i>Analysis of Measurement</i>	13
4.3. <i>Predicted condensation HTC.....</i>	13
5. Evaporation	16
5.1. <i>Dependence of Heat flux on Mass flux</i>	16
5.2. <i>Dependence of Heat flux on Temperature difference.....</i>	17
5.3. <i>Dependence of Boiling HTC on Vapour quality.....</i>	20
5.4. <i>Correlation with predicted Nusselt number.....</i>	23
6. Conclusion.....	25

1. Introduction

The historical purpose of building is protection of peoples and animals before outdoor environment. Later, this protection function of building is extended about quality of indoor climate in the building. The indoor climate in modern building is controlled by system of Heating, Ventilation and Air-Conditioning (HVAC), and this system HVAC includes heat exchanger. The most energy efficient heat exchanger uses latent heat of fluid, for example condensation heat of water steam in district heating. The latent heat of fluid is used in refrigeration system or heat pump. This technical application is based on cyclic phase change of fluid liquid-gas (evaporation) and reverse phase change gas-liquid (condensation).

This phase change liquid-gas or gas-liquid is coupled with heat transfer by nucleate boiling, convective boiling and pre/post dryout effect, according to [1]-[16]. The heat transfer by nucleate boiling is depended on superheat of wall (i.e. heat flux) and presence of active nucleation sites, more [1]-[13]. The heat transfer in liquid film between superheated wall and vapour core is performed by two-phase convection boiling. This two-phase convective boiling is depended on mass flux and vapour quality, see [3]-[13]. The dryout effect is associated with annular flow, when the liquid film is consumed and superheated wall is exposed directly to vapour core, more [8]-[16].

This boiling heat transfer by nucleate boiling, convective boiling and pre/post dryout effect is simplified for engineering design on boiling heat transfer coefficient. Therefore, the dissertation thesis is aimed at experimental analysis of boiling heat transfer in building system HVAC.

2. Boiling Heat Transfer

The condensation of water steam on cold surface is studied by Nusselt [17] since 1916. This famous researcher analytically expressed dependence of boiling heat transfer coefficient on volume amount of condensed water steam on the cold wall surface. This analytical dependence assumes smooth and uniform liquid film on plane wall surface, and then condensation heat transfer coefficient is equal to inverse function of thermal resistance of condensed water steam.

This analytical Nusselt solution is not corresponded with experimental measurement over 20 %. This analytical Nusselt solution is extended about sub-cooling of liquid condensate by Bromley [18], about non-linear temperature distribution in liquid film by Rohsenow [19], about momentum movement by Sparrow [20]-[22] and laminar downward flow of condensate by Bankoff [23] or Marschall and Lee [24]. This difference over 20 % is caused by waves on surface of liquid film, and this wave's effect improves heat transfer between vapour core and liquid film as published Kapitza [25] in 1948.

Nevertheless, this boiling heat transfer is not concluded yet. The boiling heat transfer is depended on mass flux, heat flux, inclination angle, inner diameter, surface modification etc.

2.1. Effect of Mass flux and Heat flux

The dependence of boiling heat transfer coefficient on mass flux and vapour quality is published by Jung et al. [27], Bandhauer et al. [28], Arslan and Eskin [29], Adekunle et al. [30], Aroonrat and Wongwises [31] as well as Meyer et al. [32] and

[33]. This dependence is decreased for lower mass flux (below or equal to $100 \text{ kg}\cdot\text{m}^{-2}\cdot\text{s}^{-1}$) as reported Cavallini et al. [26]. This decreased dependence of boiling heat transfer coefficient on lower mass flux is substituted by dependence on temperature difference (superheat of wall) as reported Meyer and Ewim [34].

The dependence of boiling heat transfer coefficient on heat flux for fixed mass flux is studied by Greco and Vanoli [5]. Later, Greco [7] reported about dependence of boiling heat transfer coefficient on heat flux, but only in the region with dominated nucleate boiling. The effect of low mass flux is published by Meyer et al. [32] for R134a on value $50 \text{ kg}\cdot\text{m}^{-2}\cdot\text{s}^{-1}$, by Akhavan-Behabadi et al. [40] for R134a on value $46 \text{ kg}\cdot\text{m}^{-2}\cdot\text{s}^{-1}$, by Aprea et al. [41] for R407c on value $45.5 \text{ kg}\cdot\text{m}^{-2}\cdot\text{s}^{-1}$, by Lee et al. [42] for R134a on value $35.5 \text{ kg}\cdot\text{m}^{-2}\cdot\text{s}^{-1}$, by Dalkiliç et al. [43] for R134a on value $29 \text{ kg}\cdot\text{m}^{-2}\cdot\text{s}^{-1}$, by Arslan et al. [29] for R134a on value $20 \text{ kg}\cdot\text{m}^{-2}\cdot\text{s}^{-1}$ and by Fang et al. [44] for R134a on value $10 \text{ kg}\cdot\text{m}^{-2}\cdot\text{s}^{-1}$ in year 2019.

2.2. Effect of Inclination angle

The impact of inclination angle on boiling heat transfer coefficient is published by Akhavan-Behabadi et al. [40] in range 7 – 62 % and range 40 – 56 % by Ewim et al. [34]. The lowest boiling heat transfer coefficient is reported identically for vertical downward flow. Meyer et al. [33]-[36] published impact of inclined tube ($\beta = -90^\circ$ to 90°) on condensation R134a with mass flux ($G = 50$ to $600 \text{ kg}\cdot\text{m}^{-2}\cdot\text{s}^{-1}$), heat flux ($q = 4.50$ to $6.90 \text{ kW}\cdot\text{m}^{-2}$), vapour quality ($x = 20$ to 80 %) and saturation temperature ($T = 30$ to 50 °C) in inclined smooth tube with inner diameter $D = 8.38$ mm. This boiling heat transfer coefficient for vertical downward flow is obtained in range 0.9 – $1.5 \text{ kW}/(\text{m}^2\cdot\text{K})$.

Akhavan-Behabadi et al. [37]-[40] reported impact of inclined tube ($\beta = -90^\circ$ to 90°) on evaporation R134a with mass flux ($G = 46$ to $170 \text{ kg}\cdot\text{m}^{-2}\cdot\text{s}^{-1}$), heat flux ($q = 4.56$ to $9.13 \text{ kW}\cdot\text{m}^{-2}$), vapour quality ($x = 20$ to 80%) and saturation temperature ($T = -26$ to $-2 \text{ }^\circ\text{C}$) in inclined smooth and corrugated tube with inner diameter $D = 8.9 \text{ mm}$. This boiling heat transfer coefficient for vertical downward flow is obtained in range $600 - 2500 \text{ W}\cdot\text{m}^{-2}\cdot\text{K}^{-1}$. This effect of inclination angle is increased for lower mass flux as reported Akhavan-Behabadi et al. [37], Mohseni et al. [39] and Meyer et al. [33].

2.3. Effect of Inner diameter

The impact of inner diameter on boiling heat transfer coefficient is coupled with the capillary effect and flow pattern map (since size mesoscale between macro-channel and micro-channel) as noted Thome et al. [52]. The classification of channel is based on hydraulic diameter and Mehendale et al. [53] offered classification on conventional channel ($D > 6 \text{ mm}$), macro-channel ($6 \text{ mm} \geq D > 1 \text{ mm}$), meso-channel ($1 \text{ mm} \geq D > 100 \text{ }\mu\text{m}$) and micro-channel ($100 \text{ }\mu\text{m} \geq D > 1 \text{ }\mu\text{m}$). Later, Kandlikar and Grande [54] proposed classification on conventional channel ($D > 3 \text{ mm}$), mini-channel ($3 \text{ mm} \geq D > 200 \text{ }\mu\text{m}$) and micro-channel ($200 \text{ }\mu\text{m} \geq D > 10 \text{ }\mu\text{m}$). Kew and Cornwell [14] proposed approximate physical criterion for macro-to-micro-scale, see Eq. 2.1. This critical inner diameter of macro-to-micro-scale is obtained on value $D = 5.05 \text{ mm}$ for water steam.

$$D = \sqrt{\frac{4\sigma}{g(\rho_{liq} - \rho_{gas})}} \quad (\text{Eq. 2.1})$$

This impact of inner diameter on boiling heat transfer

coefficient is reported by Yan and Lin [55] (the boiling heat transfer coefficient with inner diameter $D = 2.0$ mm is about 30 – 80 % higher than for larger pipe $D \geq 8.0$ mm), Huo et al. [56] (the boiling heat transfer coefficient in tube with inner diameter $D = 2.01$ mm is higher than in tube with inner diameter $D = 4.26$ mm) and Bandhauer et al. [28] (the boiling heat transfer coefficient increases with mass flux and vapour quality, but decrease with inner diameter).

2.4. Effect of Surface modification

The impact of surface modification on boiling heat transfer coefficient is summarized by Cavallini et al. in review [57]. Yu et al. [58] reported about increased boiling heat transfer coefficient in horizontal micro-fin tube up to 200 % in comparison with horizontal smooth tube. Aroonrat and Wongwises [31] published about dimpled tube enhances the Nusselt number about 1.3 - 1.4 times in comparison with smooth tube. Solanki and Kumar [59] reported about increased boiling heat transfer coefficient about 18 – 32 % for dimpled helically coiled tube in comparison with smooth helically coiled tube, as well as increasing about 51 – 61 % in comparison with smooth straight tube. Woodcock et al. [60] published about surface modification by Piranha Pin-Fin (PPF) and (MECH-X) for ultra-high heat flux (up to $10 \text{ MW}\cdot\text{m}^{-2}$) in electronics devices. The increased boiling heat transfer coefficient in tube with corrugated surface is reported by Akhavan-Behabadi and Esmailpour [40], Aroonrat and Wongwises [45], Laohalertdecha et al. [46] and Dalkiliç et al. [47].

3. Research Aim

The dissertation thesis is focused on heat transfer analysis of phase change process in a tubular exchanger. This phase change of fluid from liquid to gas (evaporation) or reverse phase change from gas to liquid (condensation) is applied in heating/cooling system, air-conditioning, etc. This phase change process is experimentally analysed for water steam (condensation) and refrigerants (evaporation).

- ❖ **Condensation** of water steam in tubular heat exchanger with 55 spiral micro tubes with inner diameter 3.0 mm.
- ❖ **Evaporation** of refrigerant R134a, R404a and R407c with low mass flux in vertical smooth tube with inner diameter 32 mm.

The main result of dissertation thesis is extension of current state of knowledge about boiling heat transfer. This experimentally obtained knowledge is published in scientific journal.

4. Condensation

The condensation of water steam in copper spiral micro tube with total length 1300 ± 2 mm and inner diameter 3.0 ± 0.01 mm is lower than critical inner diameter 5.05 mm. This small inner diameter increases interaction of water steam with copper surface of tube. This thermodynamics interaction is caused by surface tension in fluid. The impact of surface tension on the condensation heat transfer is analysed experimentally in bundle of 55 spiral micro tubes. Number of waves on one tube is 28 pcs. The outer surface area of spiral micro tube is $15\,904$ mm² with inner surface area $11\,928$ mm². Total outer surface area of 55 tubes is $874\,703$ mm² with total inner surface area $656\,028$ mm², see Fig. 4.1.

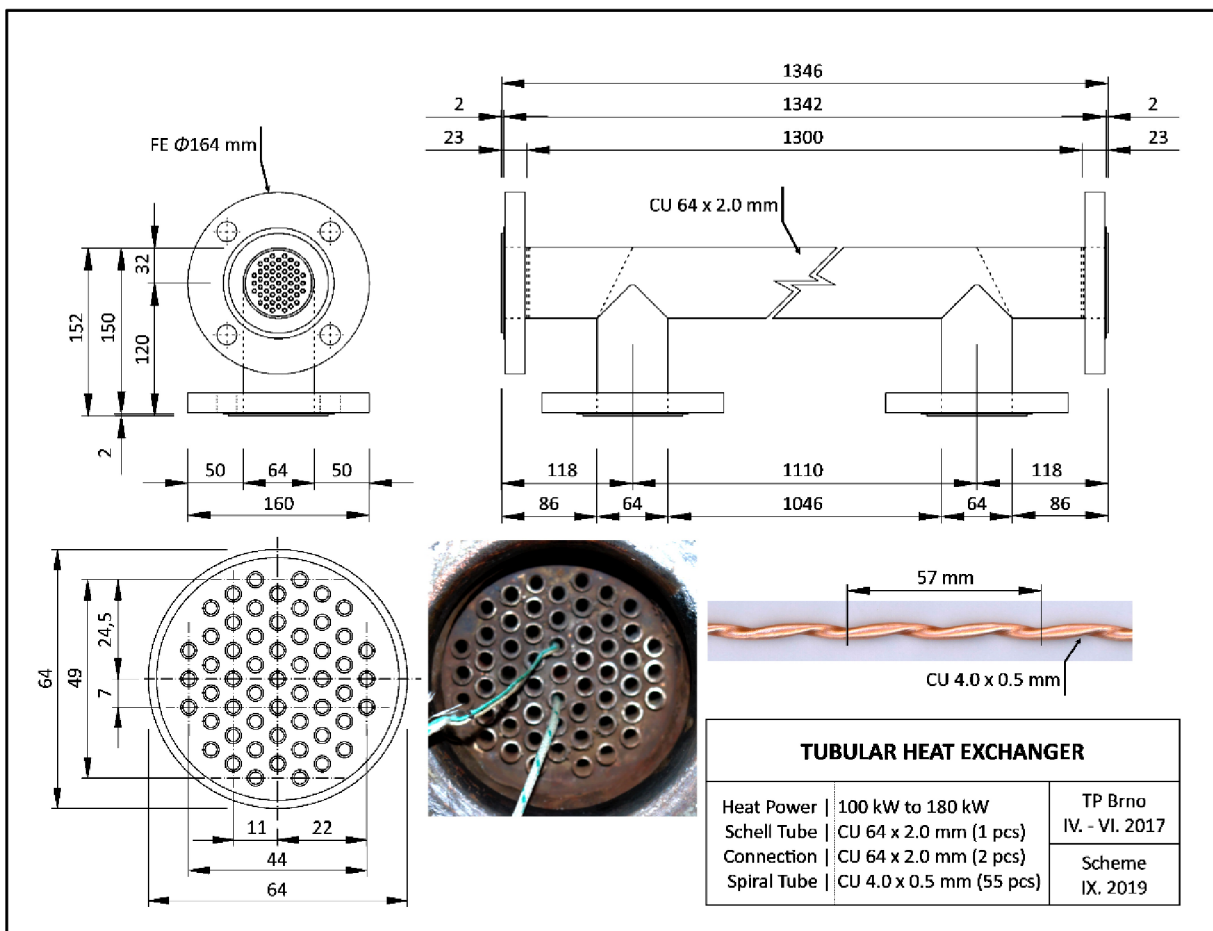


Figure 4.1 – Scheme of tubular heat exchanger with micro tubes.

4.1. Experimental Measurement

This experimental measurement is performed with mass flux of water steam in range from 0 to $1000 \text{ kg}\cdot\text{m}^{-2}\cdot\text{s}^{-1}$ and the heat flux is obtained in range from 0 to $300 \text{ kW}\cdot\text{m}^{-2}$. The vapour quality is measured in range from 0 % (total condensation) to 92% (mixture of liquid and vapour). The condensation of water steam in 55 spiral micro tubes is measured for vertical parallel-flow (11 252 data points = 15.6 hours), vertical counter-flow (12 949 data points = 17.9 hours), inclined parallel-flow (11 807 data points = 16.4 hours) and inclined counter-flow (17 171 data points = 23.8 hours), see Fig. 4.2.



Figure 4.2 – *Experimental setup of tubular heat exchanger.*

The shell of heat exchanger is insulated by Rockwool 800 76/50 mm with thermal conductivity $\lambda = 0.04 \text{ W}/(\text{m}\cdot\text{K})$. The surface temperature of shell tube below the insulation is monitored by 27 pcs thermocouples in the distance from 95 to $1209 \pm 1 \text{ mm}$.

Thermocouples are ALMEMO AHLBORN NiCr-Ni type T190-0 and T 190-1 (temperature range -25 to 400 °C), T 190-2 (temperature range -10 to 105 °C) and T 190-3 (temperature range -45 to 200 °C). Sensitivity of thermocouples is ± 0.10 K. Thermocouples on the copper surface of shell tube are glued in ultra-high thermal conductivity MasterGEL and fixed by aluminium tape. The surface temperature of shell tube is recorded by ALMEMO Multi-function data logger type 5590 in time step 5 seconds. The measurement is processed by co-author software application, see Fig. 4.3.

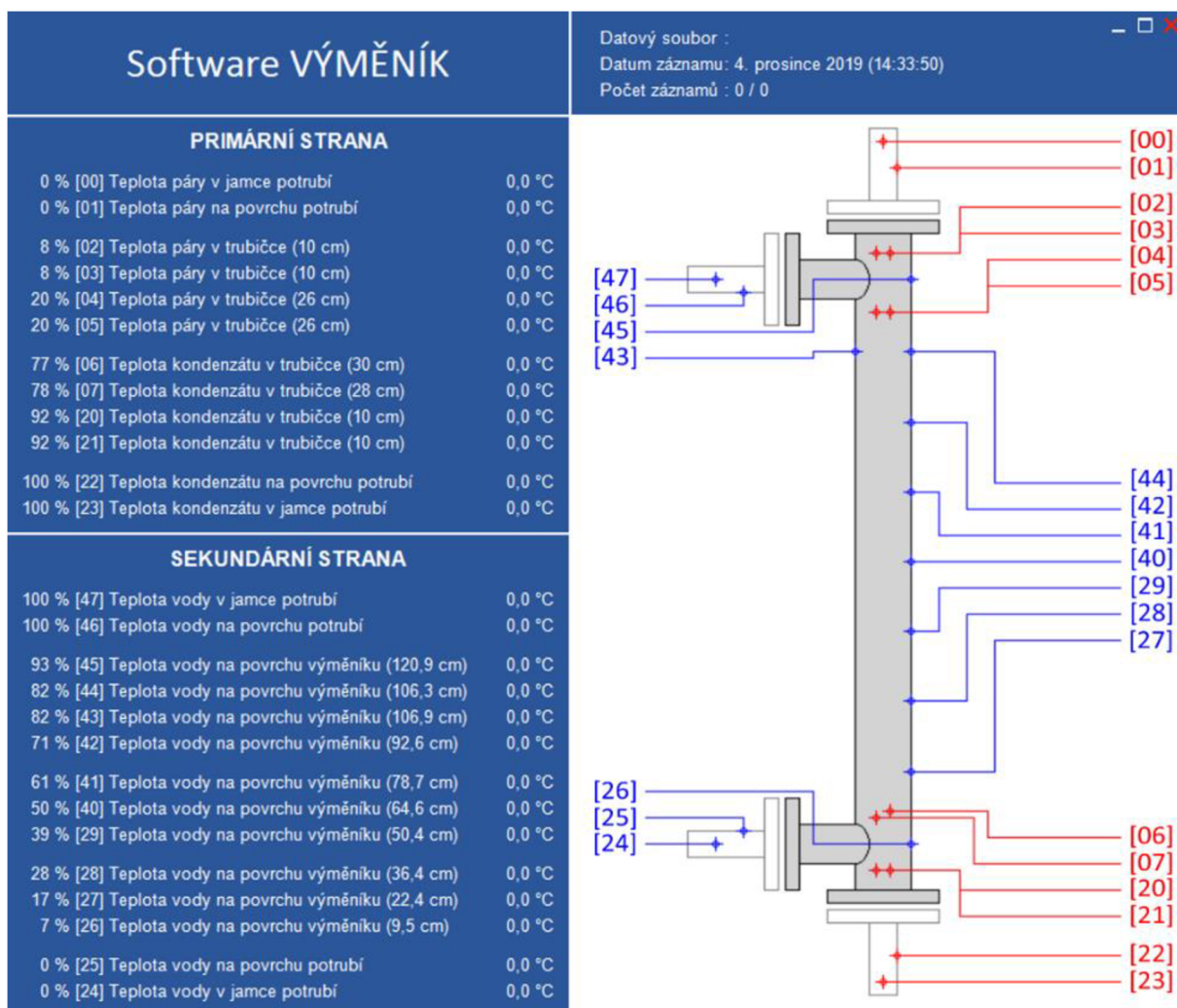


Figure 4.3 – Print-screen of own software for measurement.

4.2. Analysis of Measurement

The transferred condensation heat Q_v [W] between water steam and cooling water is calculated from (Eq. 4.1), where specific enthalpy of water steam condensate is $h_{c,out} = 419.10$ kJ/kg and condensation temperature is $t_{v,out} = 100$ °C. The logarithmic mean temperature difference ΔT [K] for counter-flow involvement is determined from (Eq. 4.2). The one-dimensional state steady overall heat transfer coefficient k [W/(m·K)] for cylindrical wall in condensing zone is calculated by (Eq. 4.3). Finally, the condensation heat transfer coefficient α_v [W/(m²·K)] is determined by Thermal resistance method and Wilson plot method.

$$Q_v = m_v \cdot (h_{v,in} - h_{c,out}) \quad (\text{Eq. 4.1})$$

$$\Delta T = \frac{(t_{v,in} - t_{w,out}) - (t_{v,out} - t_{w,in})}{\ln\left(\frac{t_{v,in} - t_{w,out}}{t_{v,out} - t_{w,in}}\right)} \quad (\text{Eq. 4.2})$$

$$k = \frac{Q_v}{n_T \cdot (L - H) \cdot \Delta T} \quad (\text{Eq. 4.3})$$

4.3. Predicted condensation HTC

The condensation heat transfer coefficient (HTC) α_v [W/(m²·K)] can be predicted by equations obtained by theoretical or experimental way. The first chosen equation is theoretically determined by Nusselt [17] in 1916. The Nusselt equation

(Eq. 4.4) is expressed from amount of condensate and thermal resistance of laminar film condensate on surface wall.

$$\alpha_v = 0.9428 \cdot \left[\frac{g \cdot \rho_c \cdot l_{23} \cdot \lambda_c^3}{\nu_c \cdot (t_v - t_T) \cdot L} \right]^{0.25} \quad (\text{Eq. 4.4})$$

The Nusselt equation (Eq. 4.4) is valid for stationary steam because flowing steam in tube causes waves on condensate surface. The wave's effect increases condensation heat transfer about 20.6 % as published Whitham [48] in (Eq. 4.5).

$$\alpha_v = 1.137 \cdot \left[\frac{g \cdot \rho_c \cdot l_{23} \cdot \lambda_c^3}{\nu_c \cdot (t_v - t_T) \cdot L} \right]^{0.25} \quad (\text{Eq. 4.5})$$

Next chosen equation (Eq. 4.6) is theoretically determined for calculation of condensation heat transfer coefficient and includes the wave's effect, too. This equation is chosen for comparison because the equation is often applied in engineering tasks. The equation (Eq. 4.6) published by Hobler [49] is valid for many kind of fluids with pressure $0.07 < p_v$ [MPa] < 17 and specific heat flux $1.0 < q_v$ [kW/m²] $< 1\ 000$.

$$\alpha_v = 0.00252 \cdot \left(\frac{\rho_v \cdot l_{23}}{\rho_c - \rho_v} \cdot \frac{\rho_c}{\sigma_c} \right)^{0.33} \cdot \frac{\lambda_c^{0.8} \cdot q_v^{0.7}}{\mu_c^{0.5} \cdot c_c^{0.167} \cdot T_v^{0.37}} \cdot p_v^{\frac{10}{T_v - 273.15}} \quad (\text{Eq. 4.6})$$

Another chosen equation (Eq. 4.7) determined by experimental way is formulated in typical exponential function $\alpha = C \cdot q^n$ similar as substitution in Wilson plot method, see (Eq. 4.7). The base of function is specific heat flux q [W/m²] and prefix constant $C = 1.537$ depends on kind of surface and fluid properties, more Kutateladze [50]. The exponent of function takes into account boundary conditions and for constant boil temperature without impact of radiation heat transfer is $n = 0.75$.

$$\alpha_v = 1.537 \cdot q_v^{0.75} \quad (\text{Eq. 4.7})$$

The last chosen equation (Eq. 4.8) for comparison is determined by experimental way and predict minimal value of Nusselt number Nu_{\min} [-] depending on fluid properties included in Prandtl number Pr_c [-]. The characteristics length d [m] in Nusselt number Nu_{\min} [-] is $d = (0.125 \cdot \nu c^2)^{0.33}$, according to Hausen [51].

$$Nu_{\min} = 0.16 \cdot Pr_c^{0.61} \quad (\text{Eq. 4.8})$$

Table 4.1 – *The correlation of obtained results with other studies*

Experimental study	D_i/L [mm]	$p_{v,in}$ [kPa]	$t_{v,in}$ [°C]	α_v $W \cdot m^{-2} \cdot K^{-1}$	ε [%]
Kubín et al. [61]	Cu 2.00/ 1285	102.2 to 185.8	100.2 to 117.9	7229	100.0
Shammari et al. [62]	Cu 28.2/ 3000	16.0 to 22.0	56.6 to 63.18	6502	89.9
Urban et al. [63]	Fe 6.50/ 1036	226.3	134.9	7285	100.8
Ma et al. [64]	Cu 30.0/ 410	100.0	100.0	6151	85.1
Kim el al. [65]	Fe 46.2/ 1800	300 to 7500	130 to 300	5443	75.3
Goodykoonz et al. (page 19) [66]	Fe 15.9/ 2133	111.7	102.2	7008	96.9
Goodykoonz et al. (page 20) [66]	Fe 15.9/ 2133	166.9	114.4	6650	92.0
Goodykoonz et al. (page 25) [66]	Fe 15.9/ 2133	266.8	129.4	8455	117.0
Goodykoonz et al. (page 29) [66]	Fe 15.9/ 2133	116.5	103.3	8920	123.4
Goodykoonz et al. (page 31) [66]	Fe 15.9/ 2133	244.1	126.7	6639	91.8
Goodykoonz et al. (page 32) [66]	Fe 15.9/ 2133	243.4	126.7	8160	112.9

5. Evaporation

The experimental analysis shows the evaporation of downward flow refrigerant R134a, R404A and R407C in the smooth vertical tube with an inner diameter 32 mm. The mass flux about $9 \text{ kg}\cdot\text{m}^{-2}\cdot\text{s}^{-1}$ in parallel/counter flow with the heating water shows suppressed dependence of heat flux on the mass flux, significant dependence of heat flux on the temperature difference, and dependence of boiling heat transfer coefficient on the vapour quality. This obtained boiling heat transfer coefficient is correlated as Nusselt numbers with the predicted Nusselt numbers.

5.1. Dependence of Heat flux on Mass flux

The dependence of local heat flux $q_{f,x}$ [$\text{kW}\cdot\text{m}^{-2}$] on the mass flux G_f [$\text{kg}\cdot\text{m}^{-2}\cdot\text{s}^{-1}$] is plotted for refrigerant R134a, R404A and R407C, see Fig. 5.1.

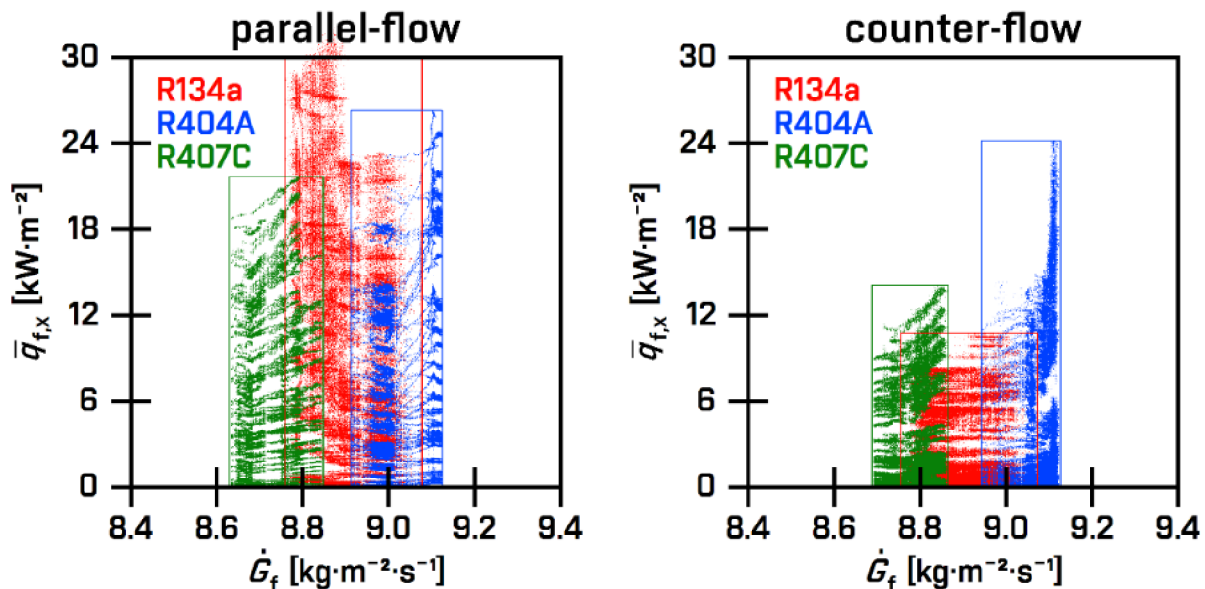


Figure 5.1 - The dependence of heat flux $q_{f,x}$ [$\text{kW}\cdot\text{m}^{-2}$] on the mass flux G_f [$\text{kg}\cdot\text{m}^{-2}\cdot\text{s}^{-1}$] is suppressed.

The refrigerant R134a in the parallel flow shows median mass flux $8.877 \pm 0.071 \text{ kg}\cdot\text{m}^{-2}\cdot\text{s}^{-1}$ and local heat flux up to $32.09 \text{ kW}\cdot\text{m}^{-2}$. The refrigerant R134a in the counter flow shows median mass flux $8.877 \pm 0.064 \text{ kg}\cdot\text{m}^{-2}\cdot\text{s}^{-1}$ and local heat flux up to $10.75 \text{ kW}\cdot\text{m}^{-2}$. The refrigerant R404A in the parallel flow shows median mass flux $9.004 \pm 0.059 \text{ kg}\cdot\text{m}^{-2}\cdot\text{s}^{-1}$ and local heat flux up to $26.34 \text{ kW}\cdot\text{m}^{-2}$. The refrigerant R404A in the counter flow shows median mass flux $9.084 \pm 0.025 \text{ kg}\cdot\text{m}^{-2}\cdot\text{s}^{-1}$ and local heat flux up to $24.20 \text{ kW}\cdot\text{m}^{-2}$. The refrigerant R407C in the parallel flow shows median mass flux $8.752 \pm 0.050 \text{ kg}\cdot\text{m}^{-2}\cdot\text{s}^{-1}$ and local heat flux up to $21.70 \text{ kW}\cdot\text{m}^{-2}$. The refrigerant R407C in the counter flow shows median mass flux $8.788 \pm 0.042 \text{ kg}\cdot\text{m}^{-2}\cdot\text{s}^{-1}$ and local heat flux up to $14.10 \text{ kW}\cdot\text{m}^{-2}$.

This low mass flux of refrigerant in the parallel flow and counter flow is comparable on 99.991 % for R134a, 99.120 % for R404A, and 99.583 % for R407C. The wide range of local heat flux for the stable mass flux is influenced by local surface temperature of evaporator tube. The temperature distribution on the inner surface of evaporator tube is driven by volume flow rate and inlet temperature of heating water in the annular space. This dependence of heat flux on the mass flux is suppressed.

5.2. Dependence of Heat flux on Temperature difference

The dependence of local heat flux $q_{f,x}$ [$\text{kW}\cdot\text{m}^{-2}$] on the temperature difference $(T_{s,x} - T_{f,x})$ [K] between the inner surface temperature of evaporator tube $T_{s,x}$ [$^{\circ}\text{C}$] and the saturation temperature of refrigerant $T_{f,x}$ [$^{\circ}\text{C}$] is plotted for refrigerant R134a, R404A and R407C, see Fig. 5.2.

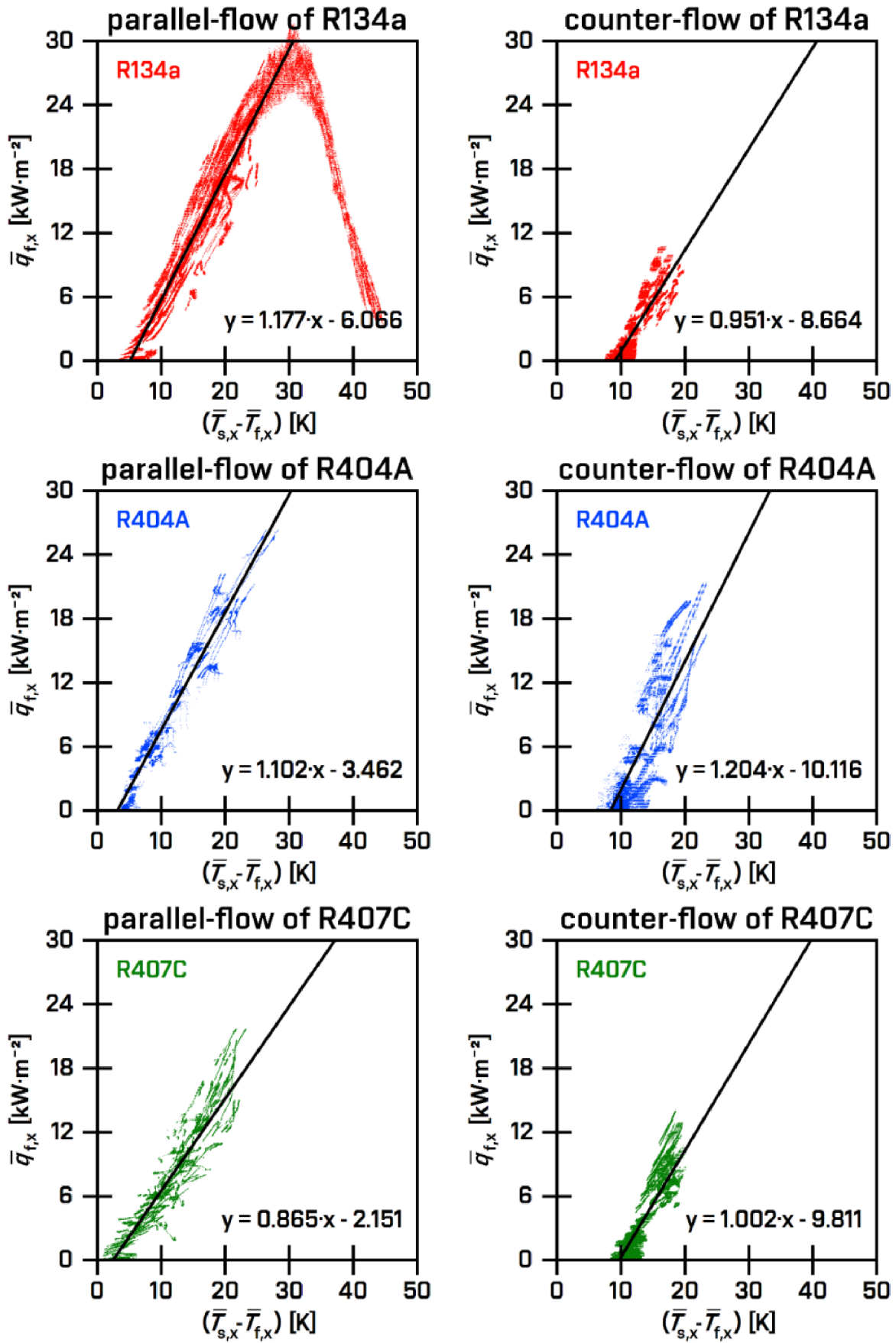


Figure 5.2 - Dependence of heat flux on temperature difference.

The refrigerant R134a with the saturation temperature $T_{f,x} \in [3.7 \text{ }^\circ\text{C}, 4.8 \text{ }^\circ\text{C}]$ shows temperature difference ($T_{s,x} - T_{f,x}$) in a range from 3.4 K to 44.9 K for the temperature of heating water $T_{w,x} \in [19.8 \text{ }^\circ\text{C}, 51.5 \text{ }^\circ\text{C}]$ in parallel flow. The linear regression of obtained result correlates on 96 % in the range from 3.4 K to 29.8 K, and the absolute difference is lower than $\pm 5.2 \text{ kW}\cdot\text{m}^{-2}$. The refrigerant R134a with the saturation temperature $T_{f,x} \in [3.1 \text{ }^\circ\text{C}, 4.7 \text{ }^\circ\text{C}]$ shows temperature difference ($T_{s,x} - T_{f,x}$) in a range from 7.3 K to 19.9 K for the temperature of heating water $T_{w,x} \in [17.1 \text{ }^\circ\text{C}, 48.1 \text{ }^\circ\text{C}]$ in counter flow. The linear regression of obtained result correlates on 90 % in the range from 7.3 K to 19.9 K, and the absolute difference is lower than $\pm 4.3 \text{ kW}\cdot\text{m}^{-2}$.

The refrigerant R404A with the saturation temperature $T_{f,x} \in [-0.5 \text{ }^\circ\text{C}, 4.4 \text{ }^\circ\text{C}]$ shows temperature difference ($T_{s,x} - T_{f,x}$) in a range from 3.5 K to 28.3 K for the temperature of heating water $T_{w,x} \in [14.8 \text{ }^\circ\text{C}, 51.6 \text{ }^\circ\text{C}]$ in parallel flow. The linear regression of obtained result correlates on 97 % in the range from 3.5 K to 28.3 K, and the absolute difference is lower than $\pm 5.1 \text{ kW}\cdot\text{m}^{-2}$. The refrigerant R404A with the saturation temperature $T_{f,x} \in [2.1 \text{ }^\circ\text{C}, 4.3 \text{ }^\circ\text{C}]$ shows temperature difference ($T_{s,x} - T_{f,x}$) in a range from 6.1 K to 23.4 K for the temperature of heating water $T_{w,x} \in [15.6 \text{ }^\circ\text{C}, 55.7 \text{ }^\circ\text{C}]$ in counter flow. The linear regression of obtained result correlates on 90 % in the range from 6.1 K to 23.4 K, and the absolute difference is lower than $\pm 8.2 \text{ kW}\cdot\text{m}^{-2}$.

The refrigerant R407C with the saturation temperature $T_{f,x} \in [-0.1 \text{ }^\circ\text{C}, 5.5 \text{ }^\circ\text{C}]$ shows temperature difference ($T_{s,x} - T_{f,x}$) in a range from 0.9 K to 23.3 K for the temperature of heating water $T_{w,x} \in [5.2 \text{ }^\circ\text{C}, 48.5 \text{ }^\circ\text{C}]$ in parallel flow. The linear

regression of obtained result correlates on 95 % in the range from 0.9 K to 23.3 K, and the absolute difference is lower than $\pm 5.7 \text{ kW}\cdot\text{m}^{-2}$. The refrigerant R407C with the saturation temperature $T_{f,x} \in [4.0 \text{ }^\circ\text{C}, 6.7 \text{ }^\circ\text{C}]$ shows temperature difference ($T_{s,x} - T_{f,x}$) in a range from 8.3 K to 20.5 K for the temperature of heating water $T_{w,x} \in [14.8 \text{ }^\circ\text{C}, 50.2 \text{ }^\circ\text{C}]$ in counter flow. The linear regression of obtained result correlates on 91 % in the range from 8.3 K to 20.5 K, and the absolute difference is lower than $\pm 6.2 \text{ kW}\cdot\text{m}^{-2}$.

This dependence of local heat flux on the temperature difference (superheated wall) is obtained by the stable low mass flux of refrigerant in combination with the variable volume flow rate of heating water with the variable inlet temperature. The obtained dependence of heat flux on the temperature difference is significant, and the dependence for the parallel flow of R134a is comparable with the Boiling curve. The variable width of dependence is the impact of measurement uncertainty. This measurement uncertainty is suppressed for the increased temperature difference.

5.3. Dependence of Boiling HTC on Vapour quality

The dependence of boiling heat transfer coefficient (HTC) $\alpha_{f,x} [\text{W}\cdot\text{m}^{-2}\cdot\text{K}^{-1}]$ on the vapour quality $X_{f,x} [-]$ is plotted for refrigerant R134a, R404A and R407C, see Fig. 5.3.

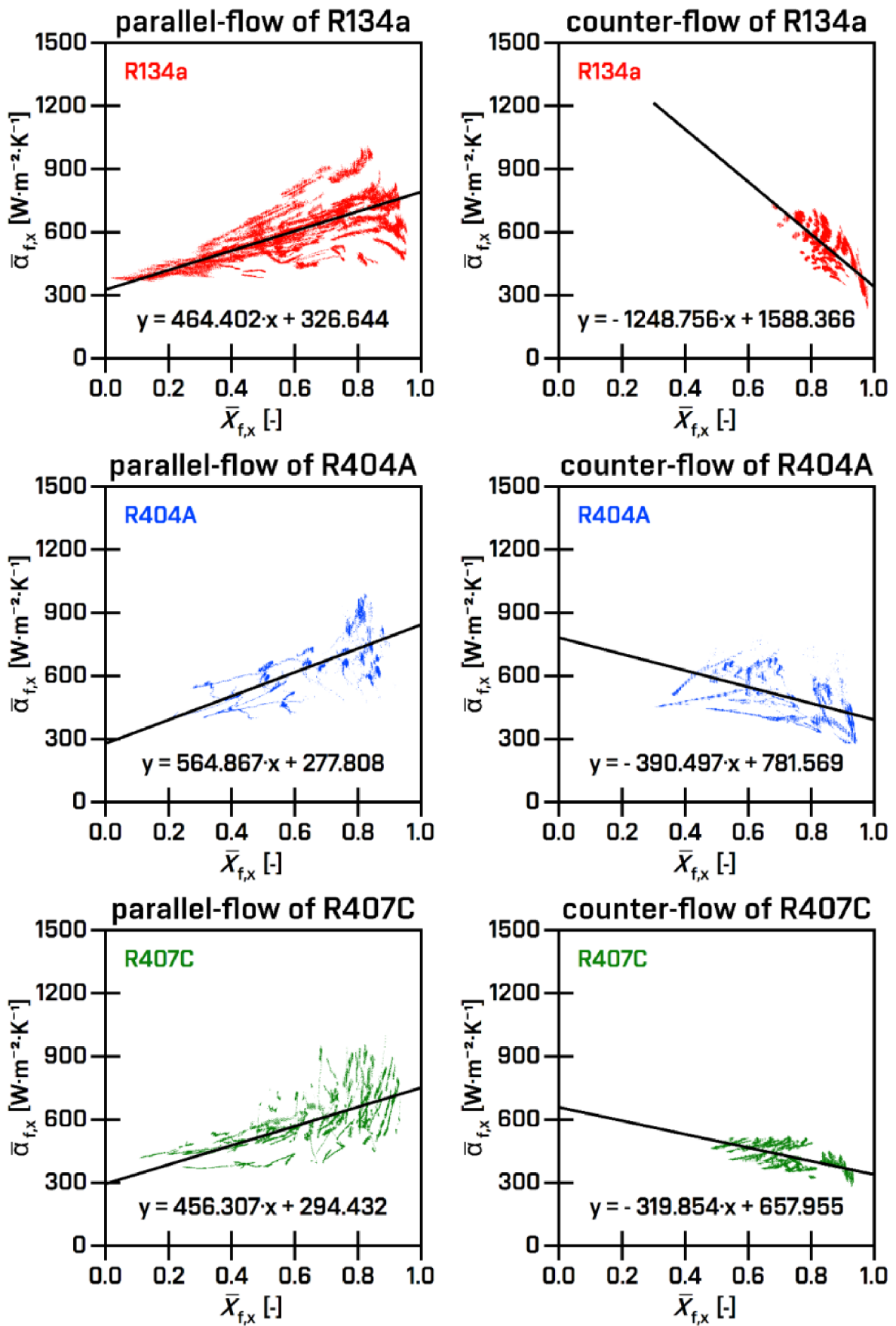


Figure 5.3 - The dependence of boiling HTC on vapour quality.

The refrigerant R134a in parallel flow with vapour quality from 1 % to 96 % shows the boiling heat transfer coefficient $609 \pm 129 \text{ W}\cdot\text{m}^{-2}\cdot\text{K}^{-1}$ in a range from 366 to $1008 \text{ W}\cdot\text{m}^{-2}\cdot\text{K}^{-1}$. The linear regression correlates with the obtained result of 71 %, and the relative deviation is lower than ± 29 %. The refrigerant R134a in counter flow with vapour quality from 68 % to 98 % shows the boiling heat transfer coefficient $518 \pm 105 \text{ W}\cdot\text{m}^{-2}\cdot\text{K}^{-1}$ in a range from 234 to $743 \text{ W}\cdot\text{m}^{-2}\cdot\text{K}^{-1}$. The linear regression correlates with the obtained result of 76 %, and the relative deviation is lower than ± 25 %.

The refrigerant R404A in parallel flow with vapour quality from 22 % to 92 % shows the boiling heat transfer coefficient $636 \pm 139 \text{ W}\cdot\text{m}^{-2}\cdot\text{K}^{-1}$ in a range from 396 to $992 \text{ W}\cdot\text{m}^{-2}\cdot\text{K}^{-1}$. The linear regression correlates with the obtained result of 73 %, and the relative deviation is lower than ± 28 %. The refrigerant R404A in counter flow with vapour quality 30 % to 94 % shows the boiling heat transfer coefficient $499 \pm 106 \text{ W}\cdot\text{m}^{-2}\cdot\text{K}^{-1}$ in a range from 278 to $794 \text{ W}\cdot\text{m}^{-2}\cdot\text{K}^{-1}$. The linear regression correlates with the obtained result of 68 %, and the relative deviation is lower than ± 36 %.

The refrigerant R407C in parallel flow with vapour quality from 11 % to 93 % shows the boiling heat transfer coefficient $573 \pm 132 \text{ W}\cdot\text{m}^{-2}\cdot\text{K}^{-1}$ in a range from 366 to $998 \text{ W}\cdot\text{m}^{-2}\cdot\text{K}^{-1}$. The linear regression correlates with the obtained result of 65 %, and the relative deviation is lower than ± 37 %. The refrigerant R407C in counter flow with vapour quality from 48 % to 93 % shows the boiling heat transfer coefficient $411 \pm 56 \text{ W}\cdot\text{m}^{-2}\cdot\text{K}^{-1}$ in a range from 281 to $524 \text{ W}\cdot\text{m}^{-2}\cdot\text{K}^{-1}$. The linear regression correlates with the obtained result of 76 %, and the relative deviation is lower than ± 21 %.

The boiling heat transfer coefficient is dependent on the vapour quality. The correlation quality of linear regression is decreased with the increased vapour quality. The dispersion of local boiling heat transfer coefficient is the complex effect of liquid drops in the vapour core, phase change of refrigerant, regime of flow, etc. The obtained dependence of local boiling heat transfer coefficient on the vapour quality is increased for the parallel flow of heating water, see Fig. 5.3.

5.4. Correlation with predicted Nusselt number

The obtained boiling heat transfer coefficient $\alpha_{f,x}$ [$\text{W}\cdot\text{m}^{-2}\cdot\text{K}^{-1}$] is compared as experimental Nusselt number Nu_{exp} [-] with the predicted Nusselt number Nu_{pre} [-], see Fig. 5.4.

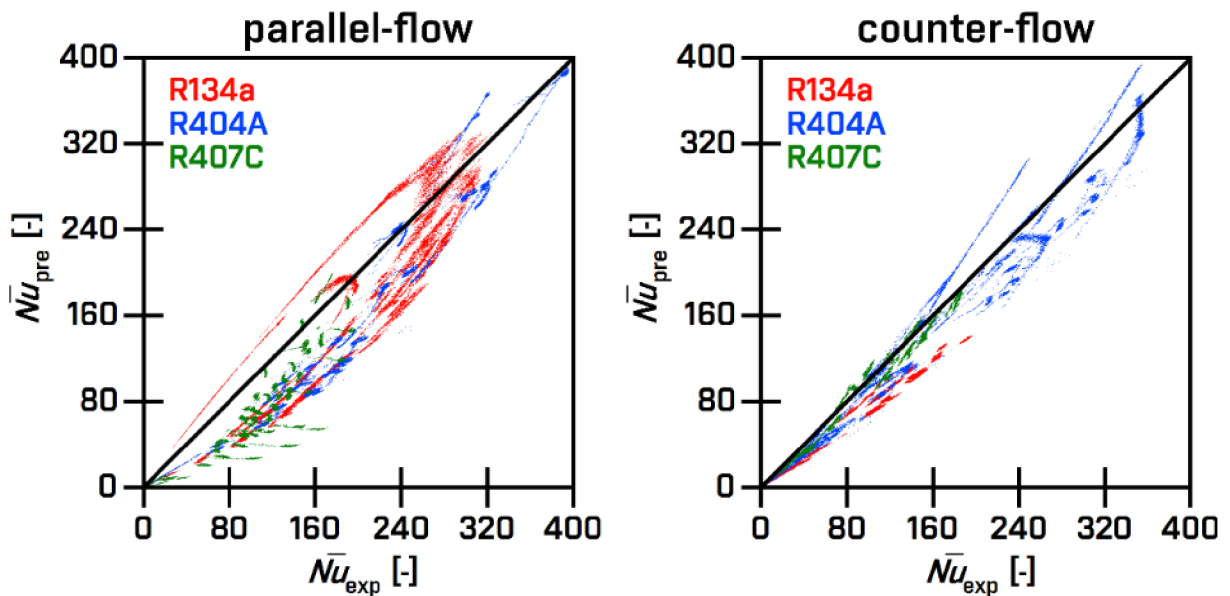


Figure 5.4 - The correlation quality of experimental Nusselt number with the predicted Nusselt numbers by Fang et al. [13].

The refrigerant R134a shows the experimental Nusselt number in the range from 1.08 to 324.1 for parallel flow and the range from 0.93 to 197.5 for counter flow. This experimental Nusselt number correlates with the predicted Nusselt number by

Fang et al. [44] on 92.2 %, Kim and Mudawar [67] on 81.1 %, and Sun and Mishima [68] on 91.1 %.

The refrigerant R404A shows the experimental Nusselt number in the range from 1.51 to 397.8 for parallel flow and the range from 0.95 to 358.4 for counter flow. This experimental Nusselt number correlates with the predicted Nusselt number by Fang et al. [13] on 92.4 %, Kim and Mudawar [67] on 86.5 %, and Sun and Mishima [68] on 89.1 %.

The refrigerant R407C shows the experimental Nusselt number in the range from 1.12 to 197.0 for parallel flow and the range from 1.02 to 187.7 for counter flow. This experimental Nusselt number correlates with the predicted Nusselt number by Fang et al. [13] on 83.2 %, Hamdar et al. [69] on 78.6 %, and Li and Wu [70] on 81.6 %.

The correlation quality of experimental Nusselt number with the predicted Nusselt number is dependent on the experimental analogy (inner diameter, mass flux, heat flux, and vapour quality). The lowest correlation on 78.6 % for R407C is obtained for the inner diameter 1.0 mm and mass flux over $200 \text{ kg}\cdot\text{m}^{-2}\cdot\text{s}^{-1}$ published by Hamdar et al. [69]. Oppositely, the highest correlation on 92.2 % for R134a and 92.4 % for R404A is obtained for the inner diameter up to 32 mm and mass flux since $10 \text{ kg}\cdot\text{m}^{-2}\cdot\text{s}^{-1}$ published by Fang et al. [13].

6. Conclusion

This dissertation thesis deals with heat and mass transfer in technical applications. The research point is an experimental analysis of heat transfer with the phase-change process in the tubular exchanger. The phase-change of fluid from liquid to gas (evaporation) or reverse phase change from gas to liquid (condensation) is used in advanced technical applications very often and therefore, this research point includes experimental analysis of condensation and evaporation process.

- ❖ **Condensation** process is studied in the tubular heat exchanger with 55 spiral micro-tubes with an inner diameter of 3.0 mm. The research method of Thermal resistance and Wilson plot is useful for analysis of experimental measurement. The boiling heat transfer coefficient is determined by theoretical, experimental, and semi-experimental prediction.
- ❖ **Evaporation** process is analysed by the low mass flux about $9 \text{ kg}/(\text{m}^2 \cdot \text{K})$ of refrigerant R134a, R404A, and R407C in the vertical smooth tube with an inner diameter of 32 mm. The obtained knowledge shows suppressed dependence of heat flux on the low mass flux, significant dependence of heat flux on the temperature difference, dependence of boiling heat transfer coefficient on the vapour quality, and correlation quality up to 92 % with the predicted Nusselt number.

Finally, this experimentally obtained knowledge of heat and mass transfer is applied in technical issues and disseminated by scientific papers.

References

- [1] Kutateladze S.S.; Boiling heat transfer; International Journal of Heat and Mass Transfer 4 (1961) 31-45; Pergamon Press, printed in Great Britain.
- [2] Thome J.R.; Boiling of new refrigerants: a state-of-the-art review; International Journal of Refrigeration 7 (1996) 435-457
- [3] Stephan K., Auracher H.; Correlations for nucleate boiling heat transfer in forced convection; International Journal of Heat and Mass Transfer 24 (1981) 99-107
- [4] Kenning D.B.R, Cooper M.G.; Saturated flow boiling of water in vertical tubes; International Journal of Heat and Mass Transfer 32 (1989) 445-458; [0017-9310/89 \$03.00+0.00]
- [5] Greco A., Vanoli G.P.; Flow-boiling of R22, R134a, R507, R404A and R410A inside a smooth horizontal tube; International Journal of Refrigeration 28 (2005) 872-880
- [6] Saitoh S., Daiguji H., Hihara E.; Correlation for boiling heat transfer of R-134a in horizontal tubes including effect of tube diameter; International Journal of Heat and Mass Transfer 50 (2007) 5215-5225
- [7] Greco A.; Convective boiling of pure and mixed refrigerants: An experimental study of the major parameters affecting heat transfer; International Journal of Heat and Mass Transfer 51 (2008) 896-909; [doi: 10.1016/j.ijheatmasstransfer.2007.11.002]
- [8] Klimenko V.V.; A generalizes correlation for two-phase forced flow heat transfer; International Journal of Heat and Mass Transfer 31 (1988) 541-552; [0017-9310/88 \$03.00+0.00]
- [9] Zürcher O., Thome J.R., Favrat D.; Evaporation of Ammonia in a Smooth Horizontal Tube: Heat Transfer Measurements and Predictions; Journal of Heat and Mass Transfer 121 (1999) 89-101
- [10] Wojtan L., Ursenbacher T., Thome J.R.; Investigation of flow boiling in horizontal tubes: Part I—A new adiabatic two-phase flow pattern map; International Journal of Heat and Mass

Transfer 48 (2005) 2955-2969

- [11] Kim S-M., Mudawar I.; Universal approach to predicting saturated flow boiling heat transfer in mini/micro-channels – Part II. Two-phase heat transfer coefficient; International Journal of Heat and Mass Transfer 64 (2013) 1239-1256
- [12] Kim S-M., Mudawar I.; Review of databases and predictive methods for heat transfer in condensing and boiling mini/micro-channel flows; International Journal of Heat and Mass Transfer 77 (2014) 627-652
- [13] Fang X., Zhuang F., Chen Ch. Wu Q., Chen Yu., Chen Ya., Yan H.; Saturated flow boiling heat transfer: review and assessment of prediction methods; International Journal of Heat and Mass Transfer 55 (2019) 197-222; [doi: 10.1007/s00231-018-2432-1]
- [14] Kew P.A., Cornwell K.; Correlations for the prediction of boiling heat transfer in small-diameter channels; Applied Thermal Engineering 17 (1997) 705-715; [1359-4311/97 \$17.00+0.00]
- [15] Lee J., Mudawar I.; Two-phase flow in high-heat-flux micro-channel heat sink for refrigeration cooling applications: Part II—heat transfer characteristics; International Journal of Heat and Mass Transfer 48 (2005) 941-955
- [16] Ribatski G., Thome J.R.; Experimental study on the onset of local dryout in an evaporating falling film on horizontal plain tubes; Experimental Thermal and Fluid Science 31 (2007) 483-493; [doi:10.1016/j.expthermflusci.2006.05.010]
- [17] Nußelt W.; Oberflächenkondensation des Wasserdampfes; Zeitschrift des Vereins Dtsch. Ingenieure. Band 60 (1916) 569
- [18] Bromley L.A.; Effect of heat capacity of condensate; Industrial and Engineering Chemistry 44 (152) 2966-2969
- [19] Rohsenow W.M.; Heat transfer and temperature distribution in laminar film condensation; Trans. ASME 78 (1956) 1645-1648
- [20] Sparrow E.M., Gregg J.L.; Laminar free convection from a vertical plate with uniform surface heat flux; Trans. ASME 78 (1956) 435-440
- [21] Sparrow E.M., Gregg J.L.; A boundary layer treatment of laminar

- film condensation; J. Heat Transfer; Trans. ASME 81 (1959) 13-18
- [22] Sparrow E.M., Marschall E.; Binary gravity-flow film condensation; J. Heat Transfer; Trans. ASME 91 (1969) 205-211
- [23] Bankoff S.G.; Stability of liquid flow down a heated inclined plane; Int. J. Heat Mass Transfer 14 (1971) 377-385
- [24] Marschall E., Lee C.Y.; Stability of condensate flow down a vertical wall; Int. J. Heat Mass Transfer 95 (1973) 41-48
- [25] Kapitsa P.L., Eksperim Zh.; Wave flow of thin layers of a viscous fluid; Teor. Fiz. 18 (1948) 3
- [26] Cavallini A., Censi G., Del Col D., Doretti L., Longo G.A., Rossetto L.; Experimental investigation on condensation heat transfer and pressure drop of new HFC refrigerants (R134a, R125, R32, R410a, R236ea) in a horizontal smooth tube; International Journal of Refrigeration 24 (2001) 73-87
- [27] Jung D., Kim C-B., Hwang S-M., Kim K-K.; Condensation heat transfer coefficients of R22, R407C, and R410A on a horizontal plain, low fin, and turbo-C tubes; International Journal of Refrigeration 26 (2003) 485-491
- [28] Bandhauer T.M., Agarwal A., Garimella S.; Measurement and modeling of condensation heat transfer coefficients in circular microchannels; ASME 128 (2006) 1050-1059
- [29] Arslan G., Eskin N.; Heat transfer characteristics for condensation of R134a in a vertical smooth tube; Experimental Heat Transfer 28 (2015) 430-445
- [30] Adelaja A.O., Dirker J., Meyer J.P.; Convective condensation heat transfer of R134a in tubes at different inclination angles; International journal of Green Energy 13 (2016) 812-821
- [31] Aroonrat K., Wongwises S.; Experimental study on two-phase condensation heat transfer and pressure drop of R-134a flowing in a dimpled tube; International Journal of Heat and Mass Transfer 106 (2017) 437-448
- [32] Meyer J.P., Ewim D.R.E.; Heat transfer coefficients during the condensation of low mass fluxes in smooth horizontal tubes; International Journal of Multiphase Flow 99 (2018) 485-499

- [33] Meyer J.P., Dirker J., Adelaje A.O.; Condensation heat transfer in smooth inclined tubes for R134a at different saturation temperatures; *International Journal of Heat and Mass Transfer* 70 (2014) 515-525
- [34] Ewim D.R.E., Meyer J.P., Noori Rahim Abadi S.M.A.; Condensation heat transfer coefficients in an inclined smooth tube at low mass fluxes; *International Journal of Heat and Mass Transfer* 123 (2018) 455-467
- [35] Lips S., Meyer J.P.; Experimental study of convective condensation in an inclined smooth tube. Part I: Inclination effect on flow pattern and heat transfer coefficient; *International Journal of Heat and Mass Transfer* 55 (2012) 395-404; [doi: 10.1016/j.ijheatmasstransfer.2011.09.033]
- [36] Lips S., Meyer J.P.; Stratified flow model for convective condensation in an inclined tube; *International Journal of Heat and Fluid Flow* 36 (2012) 83-91
- [37] Akhavan-Behabadi M.A., Mohseni S.G., Razavinasab S.M.; Evaporation heat transfer of R-134a inside a microfin tube with different tube inclinations; *Experimental Thermal and Fluid Science* 35 (2011) 996-1001
- [38] Mohseni S.G., Akhavan-Behabadi M.A., Saedinia M.; Flow pattern visualization and heat transfer characteristics of R-134a during condensation inside a smooth tube with different tube inclinations; *International Journal of Heat and Mass Transfer* 60 (2013) 598-602; [doi:10.1016/j.ijheatmasstransfer.2013.01.023]
- [39] Mohseni S.G., Akhavan-Behabadi M.A.; Flow pattern visual and heat transfer characteristics of R-134a during evaporation inside a smooth tube with different tube inclinations; *International Communications in Heat and Mass Transfer* 59 (2014) 39-45; [doi:10.1016/j.icheatmasstransfer.2014.10.018]
- [40] Akhavan-Behabadi M.A., Esmailpour M.; Experimental study of evaporation heat transfer of R-134a inside a corrugated tube with different tube inclinations; *International Communications in Heat and Mass Transfer* 55 (2014) 8-14

- [41] Aprea C., Greco A., Vanoli G.P.; Condensation heat transfer coefficients for R22 and R407C in gravity driven flow regime within a smooth horizontal tube; *International Journal of Refrigeration* 26 (2003) 393-401
- [42] Lee Ho-Saeng, Son Chang-Hyo; Condensation heat transfer and pressure drop characteristics of R-290, R-600a, R-134a and R-22 in horizontal tubes; *Heat Mass Transfer* 46 (2010) 571–584
- [43] Dalkiliç A.S., Yildiz S., Wongwises S.; Experimental investigation of convective heat transfer coefficient during downward laminar flow condensation of R134a in a vertical smooth tube; *International Journal of Heat and Mass Transfer* 52 (2009) 142-150; [doi:10.1016/j.ijheatmasstransfer.2008.05.035]
- [44] Fang X., Wu Q., Yuan Y.; A general correlation for saturated flow boiling heat transfer in channels of various sizes and flow directions; *International Journal of Heat and Mass Transfer* 107 (2017) 972–981 [doi: 10.1016/j.ijheatmasstransfer.2016.10.125]
- [45] Aroonrat K., Wongwises S.; Evaporation heat transfer and friction characteristics of R-134a flowing downward in a vertical corrugated tube; *Experimental Thermal and Fluid Science* 35 (2011) 20-28; [doi: 10.1016/j.expthermflusci.2010.08.002]
- [46] Laohalertdecha S., Dalkiliç A.S., Wongwises S.; Correlations for evaporation heat transfer coefficient and two-phase friction factor for R-134a flowing through horizontal corrugated tubes; *International Communications in Heat and Mass Transfer* 38 (2011) 1406-1413
- [47] Dalkiliç A.S., Çebi A., Acikgoz O., Wongwises S.; Prediction of frictional pressure drop of R134a during condensation inside smooth and corrugated tubes; *International Communications in Heat and Mass Transfer* 88 (2017) 183-193
- [48] G.B. Whitham, *Linear and Nonlinear Waves*, Wiley, New York, 1974.
- [49] T. Hobler, *Heat Transfer and Heat Exchangers*, Publishing House of Chemical Literature, Leningrad, 1961.
- [50] S. Kutateladze, *Theory of Heat Transfer*, Novosibirsk, 1970.

- [51] H. Hausen, Wärmeübertragung im Gegenstrom und Kreuzstrom, Berlin, 1950.
- [52] Thome J.R., El Hajal J., Cavallini A.; Condensation in horizontal tubes, part 2: new heat transfer model based on flow regimes; *International Journal of Heat and Mass Transfer* 46 (2003) 3365-3387; [doi: 10.1016/S0017-9310(03)00140-6]
- [53] Mehendale S.S., Jacobi A.M., Shah R.K.; Fluid flow and heat transfer at micro- and meso-scales with application to heat exchanger design; *Appl. Mech. Rev.* 53 (2000) 175–193; ASME Reprint No AMR290 \$18
- [54] Kandlikar S.G., Grande W.J.; Evolution of microchannel flow passages—Thermohydraulic performance and fabrication technology; *Heat Transfer Engineering* 24(2003) 3-17
- [55] Yan Y-Y., Lin T-F.; Evaporation heat transfer and pressure drop of refrigerant R-134a in a small pipe; *International Journal of Heat and Mass Transfer* 30 (1998) 4183-4194
- [56] Huo X., Chen L., Tian Y.S., Karayiannis T.G.; Flow boiling and flow regimes in small diameter tubes; *Applied Thermal Engineering* 24 (2004) 1225-1239
- [57] Cavallini A., Censi G., Del Col D., Doretti L., Longo G.A., Rossetto L., Zilio C.; Condensation inside and outside smooth and enhanced tubes — a review of recent research; *International Journal of Refrigeration* 26 (2003) 373-392
- [58] Yu M., Lin T., Tseng C.; Heat transfer and flow pattern during two-phase flow boiling of R-134a in horizontal smooth and microfin tubes; *International Journal of Refrigeration* 25 (2002)
- [59] Solanki A.K., Kumar R.; Condensation of R-134a inside dimpled helically coiled tube-in-shell type heat exchanger; *Applied Thermal Engineering* 129 (2018) 535–548
- [60] Woodcock C., Ng'oma C., Sweet M., Wang Y., Peles Y., Plawsky J.; Ultra-high heat flux dissipation with Piranha Pin Fins; *International Journal of Heat and Mass Transfer* 128 (2019) 504–515; [doi: 10.1016/j.ijheatmasstransfer.2018.09.030]
- [61] Kubín M., Hirš J., Plášek J.; Experimental analysis of steam

- condensation in vertical tube with small diameter; *International Journal of Heat and Mass Transfer* 94 (2016) 403–410
- [62] S.B. Al-Shammari, D.R. Webb, P. Heggs, Condensation of steam with and without the presence of non-condensable gases in a vertical tube, *Desalination* 169 (2004) 151–160
- [63] Urban F., Kubín M., Kučák L., Experiments on the heat exchangers with the tubes of small diameters, *AIP Conf. Proc.* 1608 (1) (2014) 245–248
- [64] X.-H. Ma, X.-D. Zhou, Z. Lan, Y.-M. Li, Y. Zhang, Condensation heat transfer enhancement in the presence of non-condensable gas using the interfacial effect of dropwise condensation, *Int. J. Heat Mass Transfer* 51 (2008) 1728–1737,
- [65] S.J. Kim, H.C. No, Turbulent film condensation of high pressure steam in a vertical tube, *Int. J. Heat and Mass Transfer* 43 (2000) 4031–4042
- [66] J.H. Goodykoontz, R.G. Dorsch, Local heat-transfer coefficients for condensation of steam in vertical downflow within a 5/8 inch diameter tube, National Aeronautics and Space Administration, Lewis Research Center (NASA), Technical Note (NASA TN D-3326), United States, Washington, D.C. 1966
- [67] S-M. Kim, I. Mudawar, Universal approach to predicting saturated flow boiling heat transfer in mini/micro-channels – Part II. Two-phase heat transfer coefficient, *International Journal of Heat Mass Transfer* 64 (2013) 1239–1256
- [68] L. Sun , K. Mishima , An evaluation of prediction methods for saturated flow boiling heat transfer in mini-channels, *Int. J. Heat Mass Transf.* 52 (2009) 5323–5329.
- [69] M. Hamdar , A. Zoughaib , D. Clodic , Flow boiling heat transfer and pressure drop of pure HFC-152a in a horizontal mini-channel, *Int. J. Refrig.* 33 (2010) 566–577.
- [70] W. Li , Z. Wu , A general criterion for evaporative heat transfer in mi- cro/mini-channels, *Int. J. Heat Mass Transf.* 53 (2010) 1967–1976.